

Ratiometric spiropyran-based fluorescent pH probe†

Qi-Hua You,^a Li Fan,^b Wing-Hong Chan,^{*a} Albert W. M. Lee^a and Shaomin Shuang^bCite this: *RSC Advances*, 2013, 3, 15762Received 25th March 2013,
Accepted 1st July 2013

DOI: 10.1039/c3ra41456f

www.rsc.org/advances

Introduction

In recent years, chemical sensors capable of measuring pH by optical methods have been widely used in analytical chemistry, physiology and the biosciences.^{1–5} Fluorescent probes have demonstrated outstanding characteristics in the detection of various analytes such as high selectivity, low detection limits, real-time detection, and high-throughput. Currently, a number of fluorophores such as rhodamine,^{6,7} fluorescein,⁸ BODIPY,^{9–11} naphthalenediimide,¹² cyanine,^{13,14} coumarin,¹⁵ and others^{16–18} have been used to design fluorescent pH probes covering the UV/Vis to NIR operation range. Amongst them, most of the sensing probes change intensity in single-emission window in response to the variation of pH. However, fluorescence signals are easily influenced by environmental factors, such as temperature, solvent polarity and the concentration of the analytes. Therefore, these factors make single-emission fluorescence detection inappropriate in the quantitation of chemical species.¹⁹

To alleviate the problems associated with single-emission measurement, the development of ratiometric measurement appears to be a valid approach. Ratiometric measurements record the fluorescence intensity at two wavelengths simultaneously and their ratio is calculated for correlating with the concentration of the analytes. As a result, ratiometric measurements can provide better accuracy by the built-in correction of two emission bands in the detection rather than that obtained by using a single wavelength. In general, several types of signal transduction mechanisms can provide ratio-

Spiropyran (SP) is an attractive molecular platform for the design of fluorescent OFF-ON probes for the detection of cations and anions operative on a ring-opening/closing mechanism. By incorporating a benzimidazole moiety at the *ortho*-position of the oxygen atom of the pyran unit, a ratiometric fluorescent probe in the NIR range for the measurement of pH change in aqueous ACN solution was designed and investigated. The ring-opening mechanism and *cis-trans* interconversion of the probe are also substantiated by ¹H NMR titration. The probe showed a ratiometric change in the pH range from 7.0 to 5.5 and the pK_a of the probe was calculated to be 5.9. The relative intensity ratio (*I*_{690 nm}/*I*_{517 nm}) changed from 0.08 to 2.11 with a more than 26-fold enhancement in response to the pH variation.

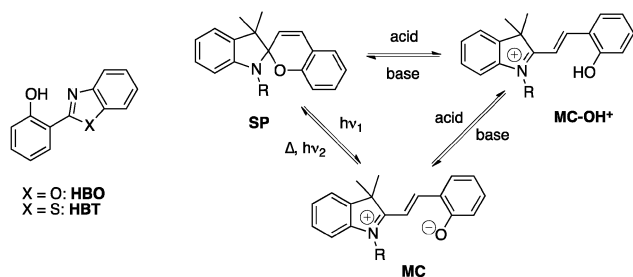
metric output: intramolecular charge transfer (ICT), fluorescence resonance electron transfer (FRET), monomer/excimer switching and excited state intramolecular proton transfer (ESIPT). Until now, a number of probes based on these mechanisms have been reported.^{20–23} Amongst them, the most remarkable photophysical property of the ESIPT probes is the large Stokes shift due to the change from the enol-form to the keto-form of the probe. For instance, *via* ESIPT, the Stokes shift of 2-(2-hydroxyphenyl)benzoxazole (HBO) and 2-(2-hydroxyphenyl)benzothiazole (HBT) could be as large as 180 nm.²⁴ Therefore, the ESIPT mechanism is an ideal strategy for the design of fluorescent probes.

Recently, more and more scientists have become interested in the design of near-infrared (NIR) fluorophoric probes due to the high penetration of NIR radiation through organic tissues and their low fluorescence background.^{25–29} Spiroyrans (SPs) are well known photochromic materials. The closed spiropyran form can transform to its ring-opened merocyanine (MC) form under photochemical irradiation.³⁰ Furthermore, spiropyran derivatives could also undergo ring-opening in the presence of acid to form MC-OH⁺ and then convert back to the SP form after the addition of base (Scheme 1).³¹ Inspired by this transformation, we hypothesized that the incorporation of the benzimidazole moiety into the *ortho*-position of the phenolate oxygen atom in the spiropyran scaffold could undergo the ESIPT process after spiropyran ring-opening in acidic conditions. Thus, a ratiometric fluorescent output for the measurement of pH in the NIR range could be achieved. Although many spiropyran-based probes for the detection of metal ions, anions and thiols have been reported,^{32–35} spiropyran-based ratiometric NIR pH probes that function in aqueous solutions, however, have been rarely exploited.³⁶

^aDepartment of Chemistry, Hong Kong Baptist University, Kowloon Tong, Hong Kong SAR, China. E-mail: whchan@life.hkbu.edu.hk; Fax: +852-3411-7348; Tel: +852-3411-7076

^bCenter of Environmental Science and Engineering Research, School of Chemistry and Chemical Engineering, Shanxi University, Taiyuan, 030006, P.R. China

† Electronic supplementary information (ESI) available. See DOI: 10.1039/c3ra41456f



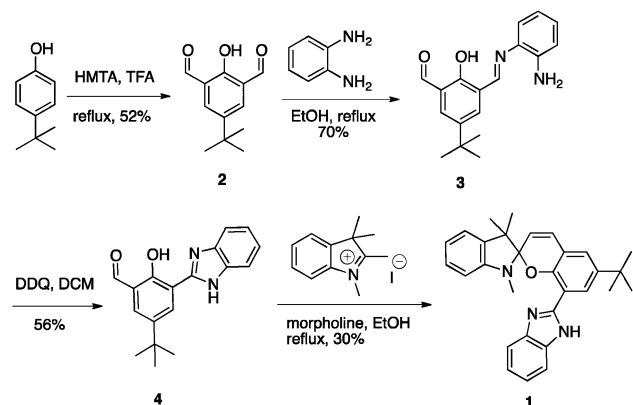
Scheme 1 Structure of HBO and HBT and reversible photochromism of spiropyran induced by thermal, photochemical and acid–base stimulation.

Results and discussion

Synthesis

As shown in Scheme 2, the synthesis of probe **1** was started from the commercially available material *tert*-butylphenol. The known procedure of diformylation of *tert*-butylphenol with hexamethylenetetramine (HMTA) in trifluoroacetic acid (TFA) gave **2** in 52% yield. The reaction of **2** with 1,2-diaminobenzene in ethanol afforded imine **3** in 70% yield. Then **3** was oxidized by DDQ to afford the strongly fluorescent compound **4** in 56% yield. In the presence of morpholine, the target product **1** was obtained in 30% yield from the reaction of **4** with 1,2,3,3-tetramethyl-3*H*-indol-1-ium iodide in ethanol. The relatively low yield of **1** was due to the strong ring-opening tendency of the spiropyran ring system in column chromatography. The resulting zwitterionic form of **1** strongly increased the polarity of the compound, thus making it difficult to be separated from impurities. All of the new compounds were well characterized by ^1H NMR, ^{13}C NMR, ESI-MS and HRMS (see Fig. S8–S10, ESI †). To facilitate the proton signal assignment in the ^1H NMR spectrum of **1**, two-dimensional H,H-COSY and H,H-NOESY experiments were performed and interacting protons of the molecule were identified (Fig. S11–S16, ESI †).

The ^1H NMR spectrum of the probe **1** (*i.e.* two signals at 1.30 and 1.34 ppm from the magnetically non-equivalent geminal methyl groups, and the spin–spin coupling constant ($J = 10.4$



Scheme 2 Synthesis of probe **1**.

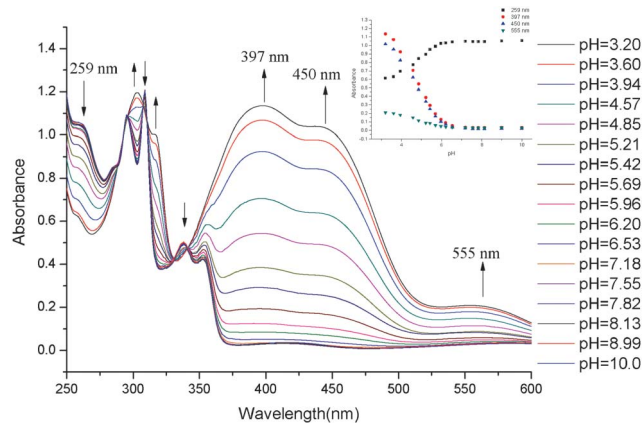


Fig. 1 Absorption spectra of **1** (50 μM) in ACN-phosphate buffer (20 mM, 1 : 1, v/v) under different pH. Inset: Plot of absorbance at 397, 450 and 545 nm of **1** (50 μM) in ACN-phosphate buffer (20 mM, 1 : 1, v/v) as a function of pH, respectively.

Hz) of the vinyl protons of the pyran moiety) unambiguously confirmed its structure that existed mainly in the spirocyclic form. 37

Photophysical properties

With the new sensing material in hand, we started to study the spectroscopic properties of probe **1** (50 μM) in ACN-phosphate buffer (20 mM, 1 : 1, v/v). As shown in Fig. 1, at a pH above 6.5, the probe showed almost no absorption in the range from 370 to 700 nm. Upon acidification of **1** from 6.5 to 4.0, the absorbance at 259, 309 and 338 nm decreased with concomitant formation of new peaks at 318, 397, 450 and 555 nm, which induced a color change of **1** from colorless to brown (Fig. S17, ESI †). Clear isobestic points at 342, 331, 311, 306 and 296 nm were observed, which indicate the acidochromic interconversion of the spirobenzopyran closed form of **1** to the extended conjugated merocyanine ring-opened form (*vide infra*).

The time course of fluorescence measurement of the probe revealed that a longer time was required to reach equilibrium in more acidic conditions (Fig. S18, ESI †). Thus, to acquire steady readings, the fluorescence spectra were collected after 30 min of incubation. The fluorescence response of probe **1** to pH was shown in Fig. 2a and 2b. A ratiometric fluorescence pattern was clearly observed under acidic conditions. Under neutral conditions, the probe showed a maximum fluorescence intensity at 517 nm ($I_{517\text{ nm}}$) due to the fluorescent spiro-form of **1** 32 and negligible fluorescence in the NIR range was observed. When pH was decreased, $I_{517\text{ nm}}$ decreased with a concomitant increase of the fluorescence intensity at 690 nm ($I_{690\text{ nm}}$). A clear isoemission point at 620 nm was observed. $I_{690\text{ nm}}$ reached its highest value at around pH 5.5. In the pH range from 7.0 to 5.5, the probe showed a ratiometric change and the ratio ($I_{690\text{ nm}}/I_{517\text{ nm}}$) changed from 0.08 to 2.11 with a more than 26-fold enhancement in the relative ratiometric intensity. When pH of the solution was decreased from 5.5 to 4.0, $I_{690\text{ nm}}$ remained almost constant while $I_{517\text{ nm}}$ was still in the decreasing trend (Fig. 2c). Under basic conditions, $I_{517\text{ nm}}$

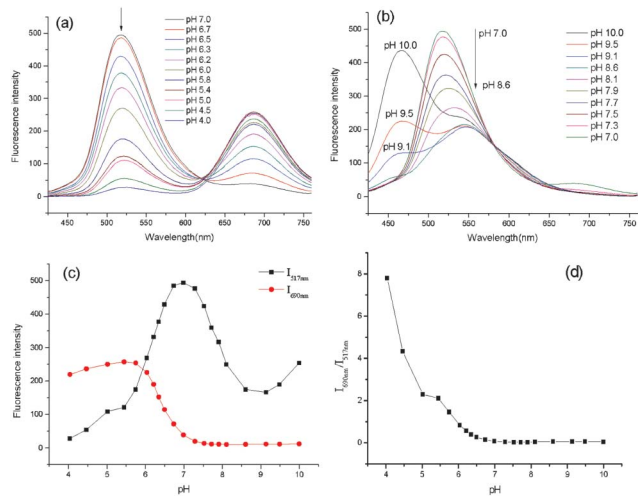


Fig. 2 Fluorescence spectra of **1** (50 μM) in ACN-phosphate buffer (20 mM, 1 : 1, v/v) in the pH range of (a) 4.0–7.0 and (b) 7.0–10.0. (c) Plot of $I_{517\text{ nm}}$ and $I_{690\text{ nm}}$ of **1** (50 μM) in ACN-phosphate buffer (20 mM, 1 : 1, v/v) as a function of pH, respectively. (d) Plot of ratio of $I_{690\text{ nm}}/I_{517\text{ nm}}$ as a function of pH.

also underwent a decreasing trend and a slightly bathochromic shift (27 nm) when the pH was increased from 7.2 to 8.6. A new hypsochromic emission at 460 nm emerged and increased significantly at a pH larger than 8.6 (Fig. 2b). Conceivably, the conformation change of the benzimidazole moiety relative to the **SP** system could trigger the observed change. The complete de-coupling of the benzimidazole and **SP** π -system could cause the hypochromic shift to 460 nm.³²

We also conducted the pH titration experiment of **1** in ACN with TFA (Fig. 3a). The changing spectral pattern was well consistent with that in aqueous ACN solution. In the absence of TFA, probe **1** showed an intense emission band at 500 nm

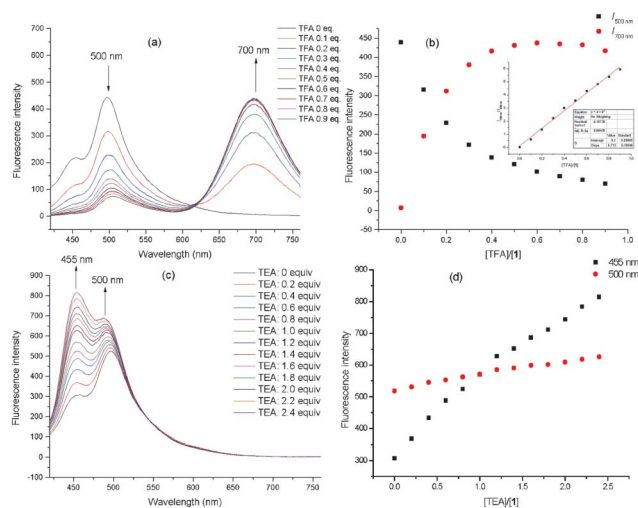


Fig. 3 (a) Fluorescence spectra of **1** (50 μM) in ACN upon the addition of TFA. (b) Plot of $I_{500\text{ nm}}$ and $I_{700\text{ nm}}$ and the ratio of $I_{700\text{ nm}}/I_{500\text{ nm}}$ (Inset) versus the ratio of $[\text{TFA}]/[\mathbf{1}]$, respectively. (c) Fluorescence spectra of **1** (50 μM) in ACN upon the addition of TEA. (d) Plot of $I_{455\text{ nm}}$ and $I_{500\text{ nm}}$ versus the ratio of $[\text{TEA}]/[\mathbf{1}]$, respectively.

and a weak band at 455 nm. Upon addition of TFA, the emission at 455 nm disappeared quickly and the emission at 500 nm decreased with concomitant increase of a new emission at 700 nm (Fig. 3a). After the addition of 0.5 equiv. of TFA, $I_{700\text{ nm}}$ did not change any more although $I_{500\text{ nm}}$ still retained in a small decreasing trend (Fig. 3b). The ratio of $I_{700\text{ nm}}/I_{500\text{ nm}}$ varied from 0.02 to 5.94 after the addition of 0.9 equiv. of TFA, with a more than 290-fold enhancement in the relative ratiometric intensity. Furthermore, the ratio of $I_{700\text{ nm}}/I_{500\text{ nm}}$ showed a linear response ($R^2 = 0.994$) to the given concentration of TFA (Fig. 3b, Inset), indicating that probe **1** could quantitatively detect H^+ concentration (0–45 μM) in ACN. The fluorescence spectral changing pattern of **1** in ACN solution upon addition of triethylamine (TEA) showed a small difference from that in aqueous ACN solution. $I_{500\text{ nm}}$ and $I_{455\text{ nm}}$ remained in a steady increasing trend upon the addition of TEA.

Based on above results, the proposed signal transduction mechanism for the fluorescent probe under acidic and basic conditions is depicted in Fig. 4. Under neutral conditions, the probe was considered to form an intramolecular hydrogen bond between the NH in the benzimidazole moiety and the oxygen atom in the spiro-pyran unit. As a consequence, rotation of the benzimidazole group was restricted and a bathochromic emission at $\sim 517\text{ nm}$ compared with that of spiro-pyran group at $\sim 475\text{ nm}$ was formed.³² The working mechanism under acidic conditions was based on the change in structure between the closed form (**SP**) and opened form (**MC-OH⁺**) mediated by protons and the ESIPT mechanism.³¹ With an increase of H^+ concentration to $\text{pH} > 5.5$ in aqueous solution or upon addition of 0–0.5 equiv. of TFA in ACN solution, in the excited state, the ring-opening of probe **1** underwent an ESIPT process from **MC-OH⁺** to **MC-NH⁺**. A proton in the oxygen atom of the phenolic group would transfer to the proximal nitrogen atom of the imine group, thus the relative position of resulting amino group and the

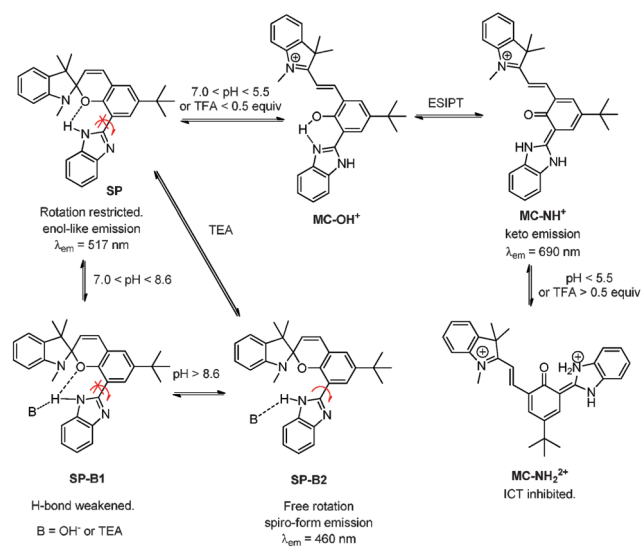


Fig. 4 Proposed ring-opening and ESIPT mechanism under acidic and basic conditions.

positively charged nitrogen atom in the keto-form MC-NH^+ are suitable for charge transfer reaction *via* π electron delocalization in the excited state.³⁸ As a result, the keto-form displaying an emission at 690 nm increased at the expense of the enol-like form emission and the pK_a of the probe was calculated to be 5.9 (Fig. S19, ESI†).¹³ The nitrogen atom of the benzimidazole moiety can be further protonated (MC-NH_2^{2+}) when $\text{pH} < 5.5$ or upon addition of >0.5 equiv. of TFA. The protonation of MC-NH^+ will inhibit the charge transfer within the molecule and reduce its fluorescence. Therefore, the emission intensity of the enol-like form kept on decreasing while the emissive peak of the keto-form decreased slowly (Fig. 2c).

Under basic conditions, the intramolecular hydrogen bond was weakened by the increasing basicity of the solution. As a result, the fluorescence intensity at 517 nm decreased gradually along with the increase of pH ($\text{SP} \rightarrow \text{SP-B1}$). At $\text{pH} > 8.6$, the hydroxyl ion present was strong enough to break the intramolecular hydrogen bond, making free rotation of the benzimidazole moiety possible. Thus, the de-coplanarity of the benzimidazole group and the spiroopyran unit caused a hypsochromic shift to 460 nm ($\text{SP-B1} \rightarrow \text{SP-B2}$). In ACN solution, probe **1** existed in an equilibrium of SP and SP-B2 forms. The addition of TEA also caused the de-coplanarity of the SP form to give the hypsochromic emission at 455 nm.

^1H NMR titration

The ring-opening mechanism was also supported by ^1H NMR titration (Fig. 5). To a solution of the probe **1** in deuteriochloroform (CDCl_3) was added sequentially portions of TFA, to a total of 3.2 equiv, followed by the addition of portions of triethylamine (TEA) to a total of 3.2 equiv., and the ^1H NMR spectrum was recorded after each addition (Fig. S20–S22, ESI†). Similar to the solution of probe **1** in ACN, **1** in CDCl_3 solution mainly existed in the spirocyclic form with intramolecular hydrogen bonding. Two far-away doublets at δ 6.69 and 7.72 ascribed to H-9 and H-12, respectively, confirmed that these two protons are in a non-equivalent chemical environment. However, the addition of small amount of TFA caused the disappearance of these two doublets and the appearance of a new broad peak at δ 7.2, suggesting the breakage of the intramolecular hydrogen bond. Thus, the free rotation of the benzimidazole moiety made the non-equivalent protons

chemically equivalent. By the addition of 0–0.6 equiv. of TFA, no obvious chemical shift change of the *N*-methyl and the *gem*-dimethyl groups was observed, indicating that the spiroopyran ring remained intact. A downfield shift of the broad peak at δ 7.2, ascribed to chemically equivalent H-9 and H-12, indicated that protonation of the imidazole moiety occurred in this stage. The formation of the imidazolium moiety (SP-H^+) also induced a small downfield shift of protons at δ 5.89, 6.67, 7.01 and 8.39 which were ascribed to H-5, H-1, H-6, and H-8 respectively. Upon further addition of 0.8–3.2 equiv. of TFA, the *gem*-dimethyl signals at δ 1.30 and 1.34 gradually coalesced to a single downshifted signal at δ 1.86, while the *N*-methyl signal at δ 2.76 disappeared with the concomitant appearance of two new singlet signals at δ 4.06 and 4.17, indicating the formation of ring-opening products comprising both *cis* and *trans* isomers (cis-MC-OH^+ and trans-MC-OH^+). Along with further addition of TFA, the intensity of the *N*-methyl resonance at δ 4.17 increased at the expense of the signal at δ 4.06. Presumably, the less stable cis-MC-OH^+ finally isomerized to trans-MC-OH^+ . At the same time, the vinyl proton H-5 doublet of the ring-closed compound at δ 5.90 (J 10.4 Hz) decreased with the concomitant increase of a new doublet signal at δ 8.59 which was attributed to the *trans*-coupled pair of H-5 (J 16.2 Hz). Also, the signals of H-1 and H-6 disappeared gradually and moved downfield to the range of δ 7.3–7.8, and the signal of H-8 underwent a small upfield shift and decrease, with the concomitant increase of a new doublet signal at δ 8.55, suggesting the conversion of the *cis*-open form to *trans*-open form. Interestingly, neutralization of the acid by the stepwise addition of portions of TEA caused a reverse change pattern of the spectra compared with that of stepwise addition of TFA to the probe, suggesting that the probe **1** is a reversible pH sensor (Fig. S22, ESI†).

Finally, we investigated the interference of metal ions on probe **1** for the pH sensing effect. As shown in Fig. 6 and Fig. S23–S25, ESI†, the fluorescence intensity values at 517 nm and 690 nm were not influenced by the addition of a large excess (>3 mM) of biologically relevant metal ions (*i.e.* Na^+ , K^+ , and Ca^{2+}) and 50 μM of various transition metal ions at pH 4.0 and 7.0, respectively. Only the presence of Cu^{2+} quenched the fluorescence completely and produced a red colored solution. It is well-known that many multifunctional spiroopyran-based probes are responsive to Cu^{2+} , displaying the characteristic red color due to the formation of the ICT complexes.³² The paramagnetic properties of Cu^{2+} , which induce intrinsic fluorescence quenching, turned off the fluorescence of the probes.³⁹ Those results imply that probe **1** might be considered as a selective fluorescent probe for pH sensing.

Conclusions

In summary, we have designed a ratiometric dual-emission pH probe **1** through the coupling of a pH-responsive spiroopyran moiety with a benzimidazole segment suitable for the ESIPT process. This probe could be used for the ratiometric measurement of pH values in a range from 7.0 to 5.5, and the pK_a of the probe was calculated to be 5.9. In the pH range

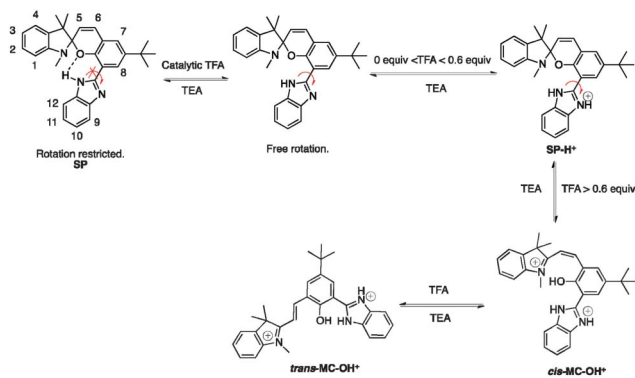


Fig. 5 Proposed structural change of probe **1** caused by the titration with TFA (0–3.2 equiv.) and TEA (0–3.2 equiv.) in CDCl_3 .

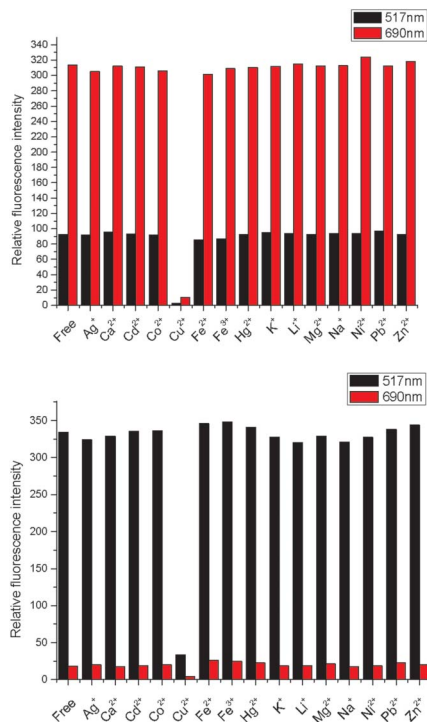


Fig. 6 Fluorescence intensity of 517 nm and 690 nm of **1** (50 μ M) in ACN-phosphate buffer (20 mM, 1 : 1, v/v) at pH 4.0 (top) and pH 7.0 (bottom) upon addition of various metal ions: Na⁺ (150 mM), K⁺ (150 mM), Ca²⁺ (3 mM), Mg²⁺ (3 mM), Li⁺ (50 μ M), Ag⁺ (50 μ M), Cu²⁺ (50 μ M), Fe²⁺ (50 μ M), Fe³⁺ (50 μ M), Zn²⁺ (50 μ M), Co²⁺ (50 μ M), Ni²⁺ (50 μ M), Cd²⁺ (50 μ M), Hg²⁺ (50 μ M), Pb²⁺ (50 μ M).

from 7.0 to 5.5, the probe showed a ratiometric change and the ratio ($I_{690\text{ nm}}/I_{517\text{ nm}}$) increased from 0.08 to 2.11 with a more than 26-fold increase in the relative ratiometric intensity. The probe could quantitatively detect H⁺ concentration (0–45 μ M) in ACN. Also, the probe suffered no interference from most of metal ions with the exception of Cu²⁺. ¹H NMR titration confirmed the reversible ring-opening/closing mechanism and *cis-trans* conversion of the spiropyran moiety.

Experimental

General

¹H NMR and ¹³C NMR spectra were recorded on a Bruker Advance-III 400 MHz Spectrometer (at 400 and 100 MHz, respectively) using trimethylsilane (TMS) as an internal standard. 2-D COSY and NOESY experiments were performed using Bruker microprograms. Low-resolution mass spectra were recorded on a Finnigan MAT SSQ-710 mass spectrometer while high-resolution mass spectra were performed using a Bruker Autoflex mass spectrometer (MALDI-TOF). Fluorescence spectra and UV-Vis spectra were collected on a PE LS50B and a Cary UV-300 spectrometer, respectively. The melting point was determined with MEL-TEMP II melting point apparatus (uncorrected). The pH measurements were performed on an Orion 420A pH mV temperature meter with a

combined glass-calomel electrode. Double-distilled water was used throughout.

All reagents for synthesis were obtained commercially and were used without further purification. Solvents such as trifluoroacetic acid (TFA), ethanol (EtOH), acetonitrile (ACN) and dichloromethane (DCM) were purchased from commercial sources and were the highest grade. Silica gel (200–300 mesh, MACHEREY-NAGEL GmbH & Co. KG) was used for column chromatography. Analytical thin-layer chromatography was performed using TLC silica gel 60 254 (aluminium sheets, Merck KGaA). In titration experiments, all the cations in the form of perchlorate or chloride and other substrates were purchased from Sigma-Aldrich, USA, and stored in a vacuum desiccator.

Sample preparation

The probe and TFA were dissolved in ACN as a stock solution (5 mM). TFA was dissolved in ACN as a stock solution (5 mM). Buffer solution was prepared by dissolving disodium hydrogen phosphate dodecahydrate in DI water (20 mM). Slight variations in the pH of the solution were achieved by adding the minimum volumes of NaOH or HCl.

Absorption and fluorescence analysis

Absorption spectra and fluorescence emission spectra were obtained with 1.0 cm quartz cells. The pH titration procedures were as follows: phosphate buffer solution (20 mM) at different pH values was mixed with ACN in a 1 : 1 ratio (v/v), then 20 μ L of stock solution was added, the mixture was equilibrated for 30 min before measurement, or 20 μ L of stock solution was added to ACN (2 mL) followed by a stepwise addition of TFA stock solution (2 μ L), and the mixture was equilibrated for 5 min before measurement. The excitation wavelength was 397 nm. The excitation and emission slits were set to 15.0 nm and 15.0 nm, respectively.

¹H NMR titration

Probe **1** (4.6 mg) was dissolved in CDCl₃ (0.5 mL) in an NMR tube. Then portions of 2.0 μ L of a solution of TFA in CDCl₃ (1.0 M) were introduced successively into the probe solution. After shaking for 1 min, the acquisition of the NMR spectrum was carried out. After the addition of 3.2 equiv. of TFA, a stepwise addition of 2.0 μ L of TEA in CDCl₃ (1.0 M) and ¹H NMR acquisition followed.

Synthesis

2,6-Diformyl-4-tert-butylphenol (2). To a solution of 4-*tert*-butylphenol (2.0 g, 13.3 mmol) in TFA (25 mL) was added hexamethylenetetramine (3.9 g, 27.8 mmol) and then the mixture was heated to reflux under N₂ atmosphere for 24 h. After cooling, the reaction mixture was poured into 6 M HCl (80 mL) and stirred for 20 min. The aqueous phase was extracted with DCM (2 \times 60 mL) and the combined organic phases were washed with 4 M HCl (2 \times 80 mL), water (80 mL) and brine (80 mL) successively, then dried over Na₂SO₄. After removal of the solvent, the residue was purified by column chromatography on silica gel (PE : EA = 40 : 1) to give a light yellow solid **2** (1.44 g, yield: 52%); m.p. 103–104 $^{\circ}$ C.⁴⁰

¹H-NMR (400 MHz, CDCl₃) δ 11.48 (1H, s), 10.25 (2H, s), 7.99 (2H, s), 1.36 (9H, s).

¹³C-NMR (100 MHz, CDCl₃) δ 192.44, 161.70, 143.14, 134.67, 122.67, 34.32, 31.10.

(*E*)-3-(((2-Aminophenyl)imino)methyl)-5-(*tert*-butyl)-2-hydroxybenzaldehyde (**3**). The mixture **2** (0.31 g, 1.5 mmol) and 1,2-diaminobenzene (0.17 g, 1.6 mmol) in absolute EtOH (20 mL) was heated to 50 °C for 6 h. After cooling, the solid was filtered and washed with small portions of EtOH to give a yellow solid **3** (0.31 g, yield: 70%); m.p.: 264–265 °C.

¹H-NMR (400 MHz, CDCl₃) δ 13.56 (1H, s), 8.63 (1H, s), 7.42 (1H, d, *J* = 2.3 Hz), 7.34 (1H, d, *J* = 2.3 Hz), 7.28–7.24 (m, 1H), 7.06 (1H, dd, *J* = 7.7 Hz, *J* = 1.4 Hz), 6.97 (1H, d, *J* = 8.1 Hz), 6.79 (1H, dt, *J* = 7.6 Hz, *J* = 1.1 Hz), 6.32 (1H, t, *J* = 5.6 Hz), 4.46 (2H, d, *J* = 5.8 Hz), 1.33 (9H, s).

¹³C-NMR (100 MHz, CDCl₃) δ 162.17, 157.25, 143.47, 141.83, 136.18, 130.90, 128.23, 128.06, 124.98, 119.16, 118.03, 117.46, 111.77, 47.28, 34.07, 31.44.

3-(1*H*-Benzo[*d*]imidazol-2-yl)-5-(*tert*-butyl)-2-hydroxybenzaldehyde (**4**). To a suspension of **3** (0.16 g, 0.5 mmol) in DCM (20 mL) was added DDQ (0.24 g, 1.0 mmol) and the reaction mixture was stirred at room temperature for 2 h. After removal of the solvent, the residue was purified by column chromatography on silica gel (PE : EA = 20 : 1) to afford **4** as a yellow solid (90 mg, 56% yield); m.p.: 249–251 °C.

¹H-NMR (400 MHz, MeOD) δ 10.42 (1H, s), 8.41 (1H, d, *J* = 2.5 Hz), 7.90 (1H, d, *J* = 2.5 Hz), 7.65–7.63 (2H, m), 7.31–7.28 (2H, m), 1.42 (9H, s).

¹³C-NMR (100 MHz, MeOD) δ 193.54, 160.38, 151.79, 143.61, 138.78, 131.79, 129.16, 124.28, 116.22, 115.87, 35.41, 31.70.

ESI-MS: *m/z* calcd for C₁₈H₁₈N₂O₂ [M + H⁺] 295.14, found, 295.3.

8-(1*H*-Benzo[*d*]imidazol-2-yl)-6-(*tert*-butyl)-1',3',3'-trimethylspiro[chromene-2,2'-indoline] (**1**). A mixture of **4** (40 mg, 0.14 mmol) and 1,2,3,3-tetramethyl-3*H*-indol-1-ium iodide (42 mg, 0.14 mmol) in absolute EtOH (10 mL) was heated to reflux under N₂ atmosphere. A solution of morpholine (24 mg, 0.28 mmol) in absolute EtOH (10 mL) was added in a dropwise manner. After addition, the reaction mixture was refluxed for 2 h. Then the solvent was evaporated under reduced pressure and the residue was purified by column chromatography on silica gel (PE : EA = 50 : 1) to afford **1** as a pink solid (19 mg, 30% yield).

¹H-NMR (400 MHz, CDCl₃) δ 9.79 (1H, s), 8.41 (1H, d, *J* = 2.4 Hz), 7.74 (1H, d, *J* = 8.1 Hz), 7.39 (1H, dt, *J* = 7.7 Hz, *J* = 1.3 Hz), 7.25 (1H, dd, *J* = 7.3 Hz, *J* = 0.8 Hz), 7.21–7.16 (2H, m), 7.12 (dt, *J* = 7.4 Hz, *J* = 0.9 Hz), 7.01 (1H, d, *J* = 10.4 Hz), 6.69 (2H, m), 5.90 (1H, d, *J* = 10.4 Hz), 2.77 (3H, s), 1.39 (9H, s), 1.34 (3H, s), 1.30 (3H, s).

¹³C-NMR (100 MHz, CDCl₃) δ 149.62, 149.51, 148.18, 143.96, 142.58, 136.79, 133.46, 131.09, 128.27, 126.49, 125.97, 122.45, 122.18, 122.03, 120.32, 119.08, 118.97, 117.93, 114.82, 110.94, 108.28, 107.40, 51.90, 34.42, 31.48, 29.55, 24.64, 19.69.

HRMS (MALDI-TOF): *m/z* calcd for C₃₉H₃₉N₅O₄ [M + H⁺] 450.2540, found, 450.2561.

Acknowledgements

The work was supported by a grant from the Research Committee of Hong Kong Baptist University (FRG2/11-12/121).

Notes and references

- J. Lakowicz, *Principles of Fluorescence Spectroscopy*, 2nd edn, Kluwer Academic/Plenum Publishers, New York, 1999, pp. 531–572.
- J.-P. Desvergne and A. W. Czarnik, *Fluorescent Chemosensors for Ion and Molecule Recognition*, Kluwer Academic Publishers, Dordrecht, The Netherlands, 1997.
- R. P. Haugland, *Molecular Probes Handbook, A Guide to Fluorescent Probes and Labeling Technologies*, 10th edn, Molecular Probes Inc., Eugene, OR, 2005, pp. 935–947.
- B. Valeur, *Molecular Fluorescence: Principles and Applications*, Wiley-VCH, Weinheim, Germany, 2002.
- R. P. Haugland and M. T. Z. Spence, *Handbook of Fluorescent Probes and Research Products*, Molecular Probes Inc., 9th edn, Eugene, OR, 2002, pp. 827–848.
- Q. A. Best, R. Xu, M. E. McCarroll, L. Wang and D. J. Dyer, *Org. Lett.*, 2010, **12**, 3219–3221.
- W. Zhang, B. Tang, X. Liu, Y. Liu, K. Xu, J. Ma, L. Tong and G. Yang, *Analyst*, 2009, **134**, 367–371.
- X. Chen, Z. Li, Y. Xiang and A. Tong, *Tetrahedron Lett.*, 2008, **49**, 4697–4700.
- S. Madhu, M. R. Rao, M. S. Shaikh and M. Ravikanth, *Inorg. Chem.*, 2011, **50**, 4392–4400.
- Y. Chen, H. Wang, L. Wan, Y. Bian and J. Jiang, *J. Org. Chem.*, 2011, **76**, 3774–3781.
- H. He and D. K. P. Ng, *Org. Biomol. Chem.*, 2011, **9**, 2610–2613.
- C. Zhou, Y. Li, Y. Zhao, J. Zhang, W. Yang and Y. Li, *Org. Lett.*, 2010, **13**, 292–295.
- B. Tang, F. Yu, P. Li, L. Tong, X. Duan, T. Xie and X. Wang, *J. Am. Chem. Soc.*, 2009, **131**, 3016–3023.
- B. Tang, X. Liu, K. Xu, H. Huang, G. Yang and L. An, *Chem. Commun.*, 2007, 3726–3728.
- X. Zhou, F. Su, H. Lu, P. Senechal-Willis, Y. Tian, R. H. Johnson and D. R. Meldrum, *Biomaterials*, 2012, **33**, 171–180.
- C. N. Carroll, B. A. Coombs, S. P. McClintock, C. A. Johnson II, O. B. Berryman, D. W. Johnson and M. M. Haley, *Chem. Commun.*, 2011, **47**, 5539–5541.
- E. Kim, S. Lee and S. B. Park, *Chem. Commun.*, 2011, **47**, 7734–7736.
- P. Song, X. Chen, Y. Xiang, L. Huang, Z. Zhou, R. Wei and A. Tong, *J. Mater. Chem.*, 2011, **21**, 13470–13475.
- A. Yayon, Z. I. Cabantchik and H. Ginsburg, *EMBO J.*, 1984, **3**, 2695–2700.
- X. Lv, J. Liu, Y. Liu, Y. Zhao, Y.-Q. Sun, P. Wang and W. Guo, *Chem. Commun.*, 2011, **47**, 12843–12845.
- L. Yuan, W. Lin, Y. Xie, B. Chen and J. Song, *Chem. Commun.*, 2011, **47**, 9372–9374.
- B. Ma, F. Zeng, X. Li and S. Wu, *Chem. Commun.*, 2012, **48**, 6007–6009.
- X. Yang, Y. Guo and R. M. Strongin, *Angew. Chem., Int. Ed.*, 2011, **50**, 10690–10693.

- 24 J. Zhao, S. Ji, Y. Chen, H. Guo and P. Yang, *Phys. Chem. Chem. Phys.*, 2012, **14**, 8803–8817.
- 25 C. Bremer, C.-H. Tung, A. J. Bogdanov and R. Weissleder, *Radiology*, 2002, **222**, 814–818.
- 26 K. Kiyose, H. Kojima and T. Nagano, *Chem.–Asian J.*, 2008, **3**, 506–515.
- 27 K. Licha and C. Olbrich, *Adv. Drug Delivery Rev.*, 2005, **57**, 1087–1108.
- 28 V. Ntziachristos, C. Bremer and R. Weissleder, *Eur. J. Radiol.*, 2003, **13**, 195–208.
- 29 D. Oushiki, H. Kojima, T. Terai, M. Arita, K. Hanaoka, Y. Urano and T. Nagano, *J. Am. Chem. Soc.*, 2010, **132**, 2795–2801.
- 30 S. V. Paramonov, V. Lokshin and O. A. Fedorova, *J. Photochem. Photobiol., C*, 2011, **12**, 209–236.
- 31 J. T. C. Wojtyk, A. Wasey, N.-N. Xiao, P. M. Kazmaier, S. Hoz, C. Yu, R. P. Lemieux and E. Buncel, *J. Phys. Chem. A*, 2007, **111**, 2511–2516.
- 32 N. Shao, J. Y. Jin, H. Wang, Y. Zhang, R. H. Yang and W. H. Chan, *Anal. Chem.*, 2008, **80**, 3466–3475.
- 33 N. Shao, J. Y. Jin, S. M. Cheung, R. H. Yang, W. H. Chan and T. Mo, *Angew. Chem., Int. Ed.*, 2006, **45**, 4944–4948.
- 34 Y. Shiraishi, S. Sumiya and T. Hirai, *Chem. Commun.*, 2011, **47**, 4953–4955.
- 35 J.-F. Zhu, H. Yuan, W.-H. Chan and A. W. M. Lee, *Org. Biomol. Chem.*, 2010, **8**, 3957–3964.
- 36 Y. P. Chan, L. Fan, Q. You, W. H. Chan and A. W. M. Lee, *Tetrahedron*, 2013, **69**, 5874–5879.
- 37 C. J. Roxburgh and P. G. Sammes, *Dyes Pigm.*, 1995, **27**, 63–69.
- 38 A. P. Demchenko and P. R. Callis, *Advanced Fluorescence Reporters in Chemistry and Biology I: Fundamentals and molecular design*, Springer Heidelberg Dordrecht London New York, 2010, pp. 250–259.
- 39 Y. Zheng, J. Orbulescu, X. Ji, F. M. Andreopoulos, S. M. Pham and R. M. Leblanc, *J. Am. Chem. Soc.*, 2003, **125**, 2680–2686.
- 40 L. F. Lindoy, G. V. Meehan and N. Svenstrup, *Synthesis*, 1998, **1998**, 1029–1032.